IEEE Access
Multidisciplinary ⋮ Rapid Review ⋮ Open Access Journal

Received 9 January 2024, accepted 28 January 2024, date of publication 7 February 2024, date of current version 29 February 2024.

Digital Object Identifier 10.1109/ACCESS.2024.3363222

RESEARCH ARTICLE

Online Nonlinear P-Q Droop Estimation of Distributed Generations Based on Kalman-Filter Algorithm to Improve Voltage Stability

SOO HYOUNG LEE[1], (Member, IEEE), DONGHEE CHOI[2], (Member, IEEE), AND SEUNG-MOOK BAEK[1], (Member, IEEE)

[1]Division of Electrical, Electronic, and Control Engineering, Kongju National University, Cheonan-si 31080, South Korea
[2]Department of Electrical and Control Engineering, Cheongju University, Cheongju-si 28503, South Korea

Corresponding authors: Donghee Choi (heechoi@cju.ac.kr) and Seung-Mook Baek (smbaek@kongju.ac.kr)

This work was supported in part by the Research Grant of Kongju National University, in 2023; and in part by Korea Institute of Energy Technology Evaluation and Planning (KETEP) Grant funded by Korean Government (MOTIE), Development of Synchronous Condenser Model and Power System Inertia Operating Technology, under Grant 20223A10100030.

ABSTRACT It is expected worldwide that the increase in renewable penetration will worsen the voltage profile in contrast to the conventional synchronous generators. This is because it is not proper to authorize all independent power producers' renewable sources to control grid voltages. Although there has been a bunch of research to improve voltage stability, each has the problem of huge computational effort, limited grid reflection, calibration, etc. Thus, the indirect voltage control by droop can be a substantial solution. Then, it is the very one of the critical issues to determine the proper droop ratio, which might be strongly non-linear due to the complexity of the power system. This paper proposes the online nonlinear P-Q droop estimation of distributed generations. It improves voltage stability, which might get worse after the connection of renewable energies or energy storage devices through inverters. First, power sensitivities between multiple P and Q are derived and used to determine the initial state of the linear P-Q droop required for the initial operation that gets data for precise estimation of the P-Q droop. Thus, it enhanced the estimation performance by reducing the required data yet without the extreme P-Q range. Then, the nonlinear P-Q droop estimation is conducted with the Kalman-filter algorithm. The performance is verified by applying it to the real distribution power system of an island in Korea. For the verification, the distribution power system is modeled at the EMT level and simulated using the power system computer-aided design and electromagnetic transient and DC (PSCAD/EMTDC^{TM}). The voltage stability was improved by the proposed nonlinear P-Q droop estimation compared to the cases using fixed droop or Q of zero.

INDEX TERMS Distributed generation, Kalman-filter algorithm, non-linear P-Q droop control, renewable energy acceptability, voltage stability.

I. INTRODUCTION

Recently, many countries have planned to reach ''net zero emissions'' by 2050, which aims to neutralize carbon emissions. It relates to the issues of global warming; to limit the temperature increase under 1.5°C, the CO_2 emissions need to achieve at most 45% level of 2010 by 2030 [1]. Previously, the Korean government publicized ''Renewable Energy 3020'', which increases the domestic renewable-energy-based generation dependency by at most 20% by 2030 [2]. To realize this policy, many issues must be discussed despite many positive aspects. One of them is the voltage profile. The renewable energy connected to the distribution system penetrates constant real power without

The associate editor coordinating the review of this manuscript and approving it for publication was Arturo Conde.

responding to grid voltage or frequency. It generally causes voltage increases so that it sometimes deteriorates voltage stability by occasionally dropping the voltages due to source disconnection.

To improve the voltage profile, a model predictive control strategy has been proposed [3]. This method uses the elements of the Jacobian matrix to estimate the Q-V relationship. Getting the Q-V relationship based on the Jacobian matrix requires power flow analysis of the entire system, which causes time delay due to substantial computational effort. Also, it needs accurate pre-information online impedances. To suppress the voltage change caused by real power penetration in the weak power system, the output impedance of the inverter has been analyzed [4]. This method shows limitations in reflecting the effect of grid impedance, which continuously changes and is hard to estimate in real time.

Many pieces of research about voltage profiles/stability have been based on droop to avoid the practical problem of obtaining accurate data. An affinely adjustable robust voltage control [5] has been based on P-Q droop. This requires huge computational effort and communication due to the droop ratio being determined by the optimization that requires optimal power flow (OPF). Pamshetti et al. have analyzed the combined impact of network reconfiguration and volt-var control devices [6]. However, the modified binary gray wolf optimization (MBGWO) they proposed is also based on the power flow analysis. A neural network-based adaptive voltage control and a distributed model-predictive-control-based secondary voltage controls have been proposed for inverter-based microgrids [7], [8]. These methods focus on secondary control, but their primary controls remain in conventional droop control. Also, many research papers report Q-V droop-based methods [9], [10], [11], [12], [13], [14]. Still, they need re-calibration between their droop ratios to ensure stability and fast response when there is a change of configuration of inverter penetration.

Several centralized methods have been proposed to solve the conventional droop-causing problems. Real-time volt/var methods adaptively change the droop ratio under external disturbances [15]. The object of this method is voltage regulation for several hours. It cannot be applied to the seconds or less time voltage control. There are many studies based on optimization algorithms. An attention-enabled multi-agent DRL method gathers information from the entire system and gives an optimal decision [16]. A distributed inter-phase coordination algorithm controls the voltage with unbalanced photovoltaic integration in low-voltage systems [17]. A two-layer volt-var control method has centralized control to optimize the droops of each photovoltaic source [18]. A study controls voltage and frequency based on an artificial neural network for islanded multi-microgrids [19]. A hierarchically coordinated voltage/var control and Multistage Multi-objective Volt/VAR Control have centralized optimization processes for PV inverters [20], [21]. Although the centralized methods can solve the droop ratio problems of the localized droop, they require massive computational effort to analyze or optimize the entire system. There is a method to mitigate the voltage deviation using both real and reactive powers [22]. Although it formulates the relationships of real and reactive powers to voltages, it is valid only in the radial system, not the mesh system.

There have been a few decentralized methods. H. P. Correa et al proposed a double pilot node decentralized voltage control of PV generators [23]. Although the method avoids the massive computational effort of the centralized one, it cannot be free from the uncertainty caused by the statistical approach. Another decentralized approach [24] requires exact line impedances, so it is useful for small grids but might be not feasible for large power systems. The existing studies are summarized in Table 1.

This paper proposes an online nonlinear P-Q droop estimation of distributed generations. It improves voltage stability, which might get worse after the connection of renewable energies or energy storage devices through inverters. To remove the requirement of extreme data, which is not expected to be obtained easily, the initial droop is selected by the power sensitivity. Also, Kalman filter-based P-Q droop estimation is used for noise rejection from both P and Q measurements.

This paper is organized as follows. Section II gives a problem formulation to establish a theoretical context. Then, Section III describes the nonlinear P-Q droop estimation for a practical application. Next, a direct bus voltage control issue is discussed in Section IV to describe why the proposed method is used. After that, the advantages of the proposed method are discussed in section IV compared to the direct bus voltage control. Finally, several case studies are discussed in Sections V and VI, and the conclusion is given in Section 8.

TABLE 1. Summary of existing studies.

Methods	Advantages	Shortcomings	Ref.
Model-Based	-Improve voltage	-Computational effort	[3]
	-Suppress variation	-Limit to reflect grid	[4]
Adjustable voltage control	-Avoid problems from inaccurate data	-Huge computational effort	[5-6]
Neural network	-Secondary control	-Primary control remained	[7-8]
Q-V droop	-Suppress voltage variation -Avoid control hunting	-Droop calibration required -Large steady-state voltage error	[9-14]
Centralized	-Adaptively changed droop	-Invalid for seconds or less	[15]
	-Decision of optimal operation point	-Huge computation effort for optimization	[16-21]
	-Small computational effort	-Only valid in a radial system	[22]
Decentralized	- Avoid huge computational effort	-Uncertainty by statistical approach -Requires accurate parameters	[23-24]

II. PROBLEM FORMULATION

Real and reactive powers from distributed generation (DG) are described in [25] as

$$P_i = \sum_{j=1}^{n} |V_i|\,|V_j|\,|Y_{ij}| \cos\left(\theta_{ij} - \delta_i + \delta_j\right) \tag{1}$$

$$Q_i = -\sum_{j=1}^{n} |V_i|\,|V_j|\,|Y_{ij}| \sin\left(\theta_{ij} - \delta_i + \delta_j\right) \tag{2}$$

where index i denotes the DG-connected bus, and index j denotes the adjacent buses. δ_j and V_j are the phase angle and voltage on bus j, respectively. θ_{ij} and Y_{ij} denote phase angle and magnitude components of the admittance matrix related to the buses i and j.

Based on (1), the derivative of P_i by $|V_i|$ is calculated by

$$\frac{\partial P_i}{\partial |V_i|} = |V_i|\,|Y_{ii}| \cos\theta_{ii} + \frac{P_i}{|V_i|} \tag{3}$$

In a general power system, both the reactive and resistive components are always included in the impedance. Then, θ_{ii} is greater than -90°. Let $\theta_{ii} = -90^{\circ} + \Delta\theta_{ii}$ in order to reformulate (3) as

$$\frac{\partial P_i}{\partial |V_i|} = |V_i|\,|Y_{ii}| \sin\Delta\theta_{ii} + \frac{P_i}{|V_i|} \tag{4}$$

where $\Delta\theta_{ii}$ is always positive. Therefore, $\partial P_i/\partial|V_i|$ is greater than zero when the DG supplies real power to the power system. In other words, the voltage of bus i increases according to the real power injection of the DG on bus i.

Based on (2), in the same manner with $\partial P_i/\partial|V_i|$, $\partial Q_i/\partial|V_i|$ is calculated by

$$\frac{\partial Q_i}{\partial |V_i|} = -|V_i|\,|Y_{ii}| \sin\theta_{ii} + \frac{Q_i}{|V_i|} \tag{5}$$

In the same manner with (4), (5) is reformulated as

$$\frac{\partial Q_i}{\partial |V_i|} = |V_i|\,|Y_{ii}| \cos\Delta\theta_{ii} + \frac{Q_i}{|V_i|} \tag{6}$$

where $\Delta\theta_{ii}$ is always positive as described before. Then, $\partial Q_i/\partial|V_i|$ is approximately $|V_i|\,|Y_{ii}| + Q_i/|V_i|$. In general power system, $|Y_{ii}|$ is very large because of small impedances. Therefore, $\partial Q_i/\partial|V_i|$ is generally positive unless Q_i is an unrealistically large negative value. In other words, the voltage increase by real power injection can be eliminated by absorbing proper reactive power, and vice versa.

Equations (1) and (2) constitute a set of nonlinear algebraic equations in terms of the independent variables, voltage magnitude, and phase angle. Expanding (1) and (2) in Taylor's series about the initial estimate and neglecting all higher-order terms results in the following matrix formula.

$$\begin{bmatrix} \Delta \boldsymbol{P} \\ \Delta \boldsymbol{Q} \end{bmatrix} = \begin{bmatrix} \boldsymbol{J}_{11} & \boldsymbol{J}_{12} \\ \boldsymbol{J}_{21} & \boldsymbol{J}_{22} \end{bmatrix} \begin{bmatrix} \Delta \boldsymbol{\delta} \\ \Delta \boldsymbol{V} \end{bmatrix} \tag{7}$$

The Jacobian matrix gives the linearized relationship between small changes in voltage angle $\Delta\delta_i$ and voltage magnitude $\Delta|V_i|$ with the small change in real and reactive power, ΔP_i and ΔQ_i. Elements of the Jacobian matrix are the partial derivatives of (1) and (2). Equation (7) can be transformed to its inverse form as (8) to focus the sub-matrices, $\boldsymbol{K}_{ij}$ of the inverse Jacobian [26].

$$\begin{bmatrix} \Delta \boldsymbol{\delta} \\ \Delta \boldsymbol{V} \end{bmatrix} = \boldsymbol{J}^{-1} \begin{bmatrix} \Delta \boldsymbol{P} \\ \Delta \boldsymbol{Q} \end{bmatrix} = \begin{bmatrix} \boldsymbol{K}_{11} & \boldsymbol{K}_{12} \\ \boldsymbol{K}_{21} & \boldsymbol{K}_{22} \end{bmatrix} \begin{bmatrix} \Delta \boldsymbol{P} \\ \Delta \boldsymbol{Q} \end{bmatrix} \tag{8}$$

Then, the voltage changes by the real and reactive power changes are

$$\Delta \boldsymbol{V} = \boldsymbol{K}_{21} \Delta \boldsymbol{P} \tag{9}$$

$$\Delta \boldsymbol{V} = \boldsymbol{K}_{22} \Delta \boldsymbol{Q} \tag{10}$$

Consequently, the reactive power is calculated as (11) for the elimination of the voltage variation caused by the real power injection.

$$\Delta \boldsymbol{Q} = -\boldsymbol{K}_{22}^{-1} \boldsymbol{K}_{21} \Delta \boldsymbol{P} = \boldsymbol{D} \Delta \boldsymbol{P} \tag{11}$$

In practice, it is very hard to achieve information of load changes or other DG generations in real-time. Therefore, it is reasonable that the DG considers the only bus that it is connected to. Equation (11) can be simplified to

$$\Delta Q_i = D_{ii} \Delta P_i = -\frac{K_{21,ii}}{K_{22,ii}} \Delta P_i \tag{12}$$

As a result, the voltage variation on bus i by the real power injection to bus i is eliminated. However, the DG on bus i does not care about other DG's power injections and load variations.

III. NONLINEAR P-Q DROOP ESTIMATION

As shown in (3) and (5), the derivatives of P_i and Q_i by $|V_i|$ are affected by P_i and Q_i, respectively. Therefore, the P_i-Q_i droop ratio is not constant, but changes according to both P_i and Q_i, so the P-Q droop ratio maintaining the V to be constant should be updated according to P_i and Q_i. It results in a nonlinear relationship between the real and reactive powers even if the voltage magnitude of $|V_i|$ is maintained constant. In other words, the P-Q droop ratio of D_{ii} requires recalculation according to the changes of P_i and Q_i, so it might require huge computational efforts during the system operation. The P-Q droop accuracy can be improved without a huge increase in computational effort by estimating the nonlinear relationship. To get an accurate nonlinear P-Q droop curve, the estimation must be conducted using measured data while the measurement errors are effectively removed. To deal with this problem, the online P-Q droop curve estimation algorithm is studied based on the Kalman filter algorithm. The Kalman filter algorithm [27], [28], [29] has excellent smoothing properties and the noise rejection capability robust to the process and measurement noises. In practical environments (in which the states are driven by process noise and observation is made in the presence of the measurement noise), the P-Q droop curve can be formulated with a linear time-varying state equation.

In this study, the state model applied for the estimation is given as

$$\begin{aligned} \mathbf{x}(t+\Delta t) &= \mathbf{\Phi x}(t) + \mathbf{\Gamma \omega}(t), \mathbf{x}(0) = \mathbf{x}_0 \\ \mathrm{y}(t) &= \mathbf{c}(t) \cdot \mathbf{x}(t) \\ \mathrm{z}(t) &= \mathrm{y}(t) + \mathrm{v}(t) \end{aligned} \tag{13}$$

where the matrices, $\mathbf{\Phi}(\in \mathrm{R}^{n\times n})$, $\mathbf{\Gamma}(\in \mathrm{R}^{n\times m})$, and vector $\mathbf{c}(\in \mathrm{R}^{1\times n})$ are known deterministic variables, and the identity matrix, $\mathbf{I}(\in \mathrm{R}^{n\times n})$, is usually chosen for the matrix, $\mathbf{\Phi}$. The state vector, $\mathbf{x}(\in \mathrm{R}^{n\times 1})$ represents the weight vector. And, $\boldsymbol{\omega}(\in \mathrm{R}^{m\times 1})$ is the process noise vector, z is the measured output, and v is the stationary measurement noise. Then, the estimate of the state vector is updated by using the following steps:

- Measurement update: Acquire the measurements, $\mathrm{z}(t)$ and compute a *posteriori* quantities.

$$\begin{aligned} \mathbf{k}(t) &= \mathbf{P}^{-}(t)\mathbf{c}(t)^T \left[\mathbf{c}(t)\mathbf{P}^{-}(t)\mathbf{c}(t)^T + r\right]^{-1} \\ \hat{\mathbf{x}}(t) &= \hat{\mathbf{x}}^{-}(t) + \mathbf{k}(t)\left[\mathrm{z}(t) - \mathbf{c}(t)\hat{\mathbf{x}}^{-}(t)\right] \\ \mathbf{P}(t) &= \mathbf{P}^{-}(t) - \mathbf{k}(t)\mathbf{c}(t)\mathbf{P}^{-}(t) \end{aligned} \tag{14}$$

  where $\mathbf{k}(\in \mathrm{R}^{n\times 1})$ is the Kalman gain, $\mathbf{P}(\in \mathrm{R}^{n\times n})$ is a positive-definite symmetric matrix, and r is a positive number selected to avoid a singular matrix. Typically, $\mathbf{P}^{-}(0)$ is given as $\mathbf{P}^{-}(0) = \lambda \mathbf{I}(\lambda > 0)$, where $\mathbf{I}$ is an identity matrix.
- Time update:

$$\begin{aligned} \hat{\mathbf{x}}^{-}(t+\Delta t) &= \mathbf{\Phi}\hat{\mathbf{x}}(t) \\ \mathbf{P}^{-}(t+\Delta t) &= \mathbf{\Phi P}(t)^T + \Gamma \mathbf{Q} \mathbf{\Gamma}^T \end{aligned} \tag{15}$$

  where $\mathbf{Q}(\in \mathrm{R}^{m\times m})$ is a positive-definite covariance matrix, which is zero in this study because the stationary process and measurement noises are mutually independent.
- Time increment: Increment t and repeat.
  Thereafter, the estimated output, $\hat{y}$ is calculated as

$$\hat{\mathrm{y}}(t) = \mathbf{c}(t) \cdot \hat{\mathbf{x}}(t) \tag{16}$$

The P-Q relationship is estimated by the voltages, and real and reactive powers measured from the DG-connected bus.

The matrices, $\mathbf{c}(t)$ and $\mathrm{z}(t)$ are determined by

$$c(t) = \left[1, P(t), \cdots, P(t)^n, Q(t)\right] \tag{17}$$

$$\mathrm{z}(t) = \Delta V(t) \tag{18}$$

where ΔV is the voltage deviation from the original voltage without the DG connection. Next, the estimated state, $\hat{x}(t)$ is determined by the Kalman-filter algorithm described in (14) and (15) as

$$\hat{\mathbf{x}}(t) = [\alpha_0, \alpha_1, \cdots, \alpha_n, \beta]^T \tag{19}$$

Therefore, the estimated voltage deviation is

$$\hat{\mathrm{y}}(t) = \alpha_0 + \sum_{i=1}^{n} \alpha_i P(t)^i + \beta Q(t) \tag{20}$$

To make the voltage deviation zero, the reactive power is determined by

$$Q(t) = -\frac{\alpha_0}{\beta} - \frac{1}{\beta}\sum_{i=1}^{n} \alpha_i P(t)^i \tag{21}$$

where α_0/β reflects the effects of external factors. This is because the reactive power must be zero when the real power injection of the DG is zero. Therefore, the required reactive power is determined by (22) when the external factors (i.e. other DGs and loads, etc.) are neglected.

$$Q(t) = -\frac{1}{\beta}\sum_{i=1}^{n} \alpha_i P(t)^i \tag{22}$$

As a result, the reactive power is determined instantly according to the amount of the real power injection.

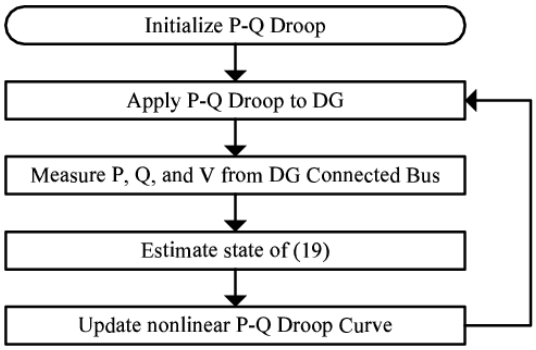

FIGURE 1. Block diagram to estimate nonlinear P-Q droop curve based on Kalman-filter algorithm.

The entire estimation algorithm is shown in Fig. 1. First, the initial P-Q droop is determined by the equation of (12). Then, P, Q, and V data are measured from the DG-connected bus by operating the DG based on the initial P-Q droop. Next, the state of (19) is estimated by (14) and (15) using (17) and (18). After that, the required reactive power is determined by (22). Finally, P, Q, and V data are measured again by operating the DG based on the updated nonlinear P-Q droop. The process repeats.

IV. DIRECT BUS VOLTAGE CONTROL ISSUE

So far, the P-Q droop focused on the single bus voltage control. However, the initial P-Q droop of (11) looks also feasible for the multiple bus voltage control. Based on that, it will be discussed why voltage fluctuations caused by external factors should not be compensated. In other words, the bus voltages should not be directly controlled.

For the explanation, a real island power system in Korea is used as shown in Fig. 2. Its operating conditions are given in Table A.I in Appendix. The rated voltage and size of the original system are 6.9kV and 1MVA, and it is powered by several diesel generators which are connected to two 6.6/6.9kV transformers. Considering the number of buses, 37 in the island power system, the maximum dimension of matrix $\boldsymbol{D}$ in (11)

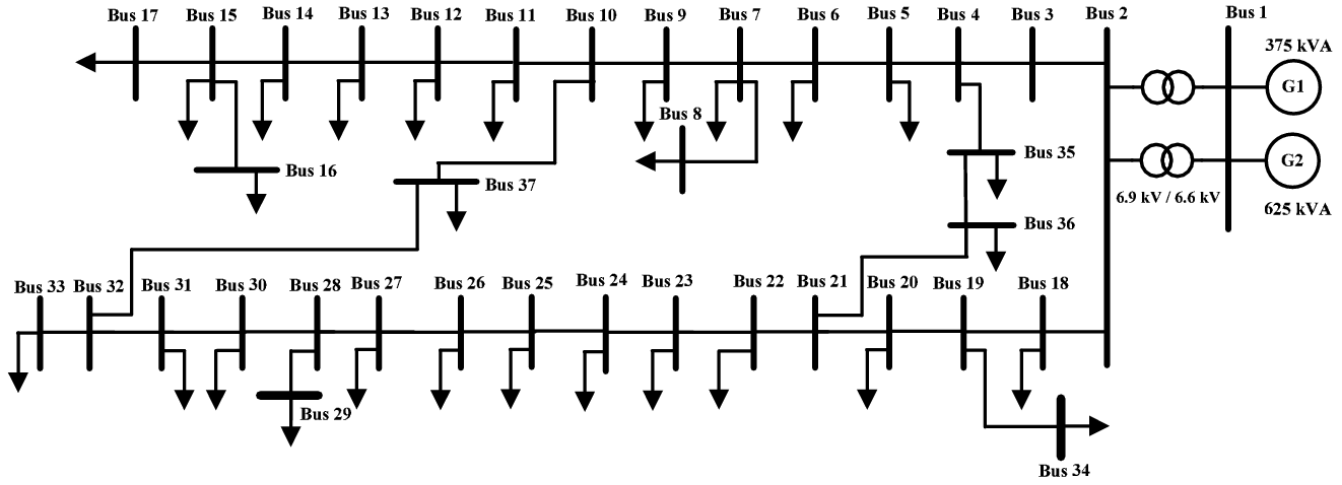

FIGURE 2. Base case model with 37 buses composed of real island power system data in Korea.

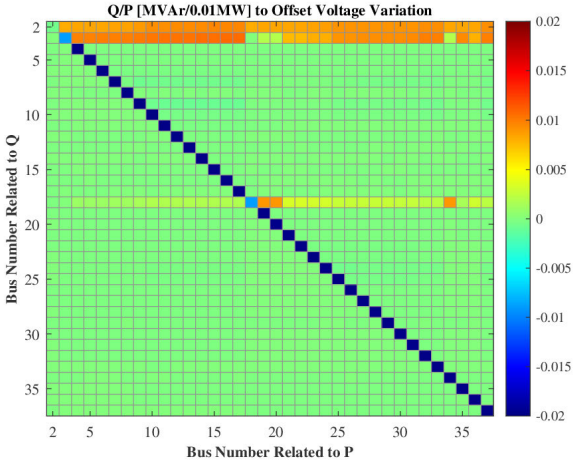

FIGURE 3. Reactive power heatmap to offset voltage variation caused by real power injection of 0.01MW from each 36 bus.

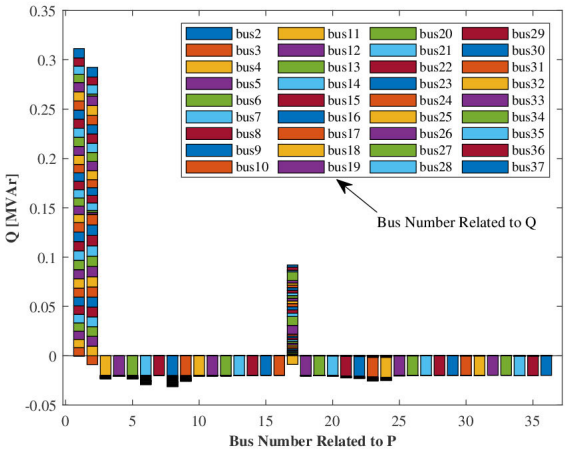

FIGURE 4. Stacked reactive power offset voltage variation caused by real power injection of 0.01MW from each 36 bus.

must be 36×36 excluding slack bus. Also, the actual dimension of matrix $\boldsymbol{D}$ is related to the number of bus voltages to be controlled as described in (9)-(11).

Assume that all 36 bus voltages are under control to be maintained constant. Then, the dimension of matrix $\boldsymbol{D}$ must be 36×36, and the reactive power requirement of each bus is affected by not only its real power injection but also those of all the other buses. It is shown in Fig. 3 that the heatmap of reactive powers to offset the voltage variation caused by real power injection of 0.01MW from each 36 bus.

The required reactive power varies from -0.0201MVAr to 0.0107MVAr depending on the buses. The net values of the reactive power injections are determined by the sum of row components of Fig. 3. That is, the required reactive powers can be simply shown using a stacked bar graph as shown in Fig. 4. The detailed description will be followed by focusing on the required reactive power generation on bus 2. The blue part on the top of the bar graph is the required reactive power to suppress the voltage variation caused by the real power injection from bus 37. In the same manner, the red part beneath the blue one is the required reactive power to suppress the effect of real power injection from bus 36. In this base case model, as a result, the DGs on buses 2 and 3 must supply about thirty times larger reactive powers than their real power injections. Also, the DGs on buses from 4 to 37 (except 17) must absorb reactive power those are larger than their real power injections. The DG on bus 17 must supply more than nine times greater reactive power than its real power injection. In this severe condition, all of the bus voltages are maintained constant unless there is a load change. In other words, the DGs are forced to be under severe situations if they directly control the bus voltages.

From the result, the system condition can be guessed briefly. The real power injection increases most of the bus voltages, so reactive power absorption is required. That reactive power absorption causes an excessive voltage drop on buses 2, 3, and 17. Therefore, reactive powers are supplied from those buses to complement the voltage drop. The sum

of negative reactive power is −0.7127MVAr which differs from the sum of the entire reactive power, −0.0354MVAr. In other words, most of the supplied and absorbed reactive powers eliminate each other to control all of the bus voltages to be constant. Therefore, it might be effective to reduce the number of controlled buses to solve the excessive reactive power supply and absorption problem.

In general, it is not reasonable to supply or absorb huge reactive power that is much greater than the real power of DG as shown in Fig. 4. To reduce the supplied and absorbed reactive powers, only two buses 9 and 23 are selected to be controlled. The heatmap in Fig. 5 shows the required reactive powers to complement the voltage variations. The left top value means that bus 9 must absorb 0.0146MVAr of reactive power due to its real power penetration of 0.01MW. In the same manner, the right top value means that bus 9 must supply 0.0055MVAr of reactive power due to the real power penetration of 0.01MW from bus 23. Therefore, the required net reactive powers of buses 9 and 23 are −0.0091MVAr and −0.004MVAr, respectively.

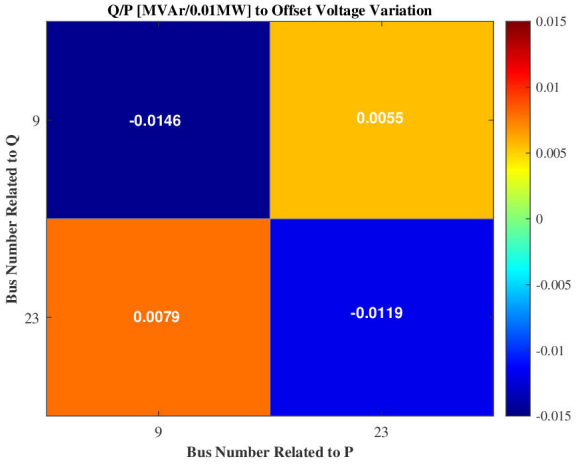

FIGURE 5. Reactive power heatmap to offset voltage variations of buses 9 and 23 caused by the real power injection of 0.01MW from bus 9 and 23 each.

Although the required reactive powers are quite smaller than those in Fig. 4, the voltages of buses 9 and 23 cannot be maintained constant if there is at least one DG on the other buses. In other words, the number of voltage-controlled buses and the required reactive power are in a trade-off relationship. Therefore, considering minimal reactive power, and data transfer between DGs, voltage fluctuations caused by the other DGs or loads should not be compensated. In other words, the bus voltages should not be directly controlled. As a result, equation (12) gives the best results to minimize the required reactive power.

V. CASE STUDIES WITH LINEAR P-Q DROOP

The initial P-Q droop ratio, D_{ii} of the base case model in Fig. 2 is calculated as shown in Table 2. Several case studies are carried out based on those droop ratios to verify the proposed method. To include the noises that are included in the real power system, at most 0.25MW white Gaussian noises are applied to the real power generation of DG.

TABLE 2. P-Q droop ratio of each bus (VAr/W).

Bus	Q/P	Bus	Q/P	Bus	Q/P	Bus	Q/P
2	-0.0565	11	-1.1965	20	-0.2608	29	-1.2992
3	-0.0656	12	-1.2387	21	-0.3433	30	-1.2525
4	-0.1891	13	-1.2767	22	-0.3799	31	-1.2540
5	-0.2456	14	-1.3126	23	-0.7808	32	-1.2596
6	-0.2981	15	-1.3455	24	-0.8769	33	-1.3865
7	-0.5796	16	-1.4340	25	-1.2208	34	-0.6587
8	-0.8112	17	-1.3815	26	-1.2331	35	-0.2322
9	-0.9424	18	-0.0650	27	-1.2468	36	-0.3340
10	-1.1515	19	-0.2574	28	-1.2489	37	-1.2583

A. P-Q DROOP-BASED SINGLE DG

To verify the effectiveness of the proposed method for a single DG-connected system, a DG is connected to bus 23 in the base case model of Fig. 2. The real and reactive powers change from zeros to 1MW and -0.7808MVAr based on the P-Q droop of bus 23, respectively. In the case of controlled simulation, only real power changes from zeros to 0.5MW, and the reactive power is maintained at zero. As shown in Fig. 6, the increased voltage up to 1.065pu in the controlled simulation is resolved by the reactive power absorption based on the P-Q droop. In the case of large real power penetration, however, the voltage variation is changed to negative (i.e., below the dashed line). That is, the adequate P-Q droop is not linear but complex. This is why the nonlinear P-Q droop curve requires to be estimated. Nevertheless, the initial P-Q droop is meaningful in itself reducing the voltage variation. This is because many more samples and extreme case samples are required if the initial P-Q droop is unknown [30].

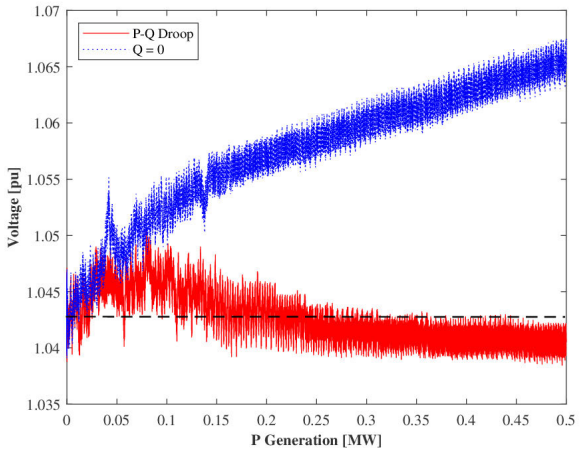

FIGURE 6. Voltage variations on bus 23 according to the real power injection using P-Q droop control (red solid line) and Q=0 (blue dotted line).

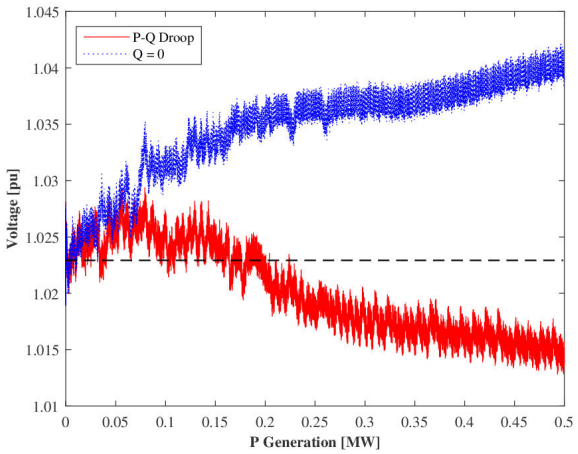

FIGURE 7. Voltage variations on bus 9 according to the total real power injection using P-Q droop control (red solid line) and Q=0 (blue dotted line).

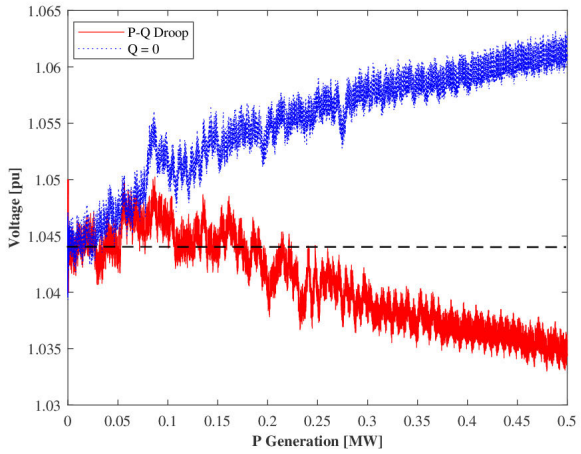

FIGURE 8. Voltage variations on bus 23 according to the total real power injection using P-Q droop control (red solid line) and Q=0 (blue dotted line).

B. P-Q DROOP BASED TWO DGs

The P-Q droop ratios in Table 2 are calculated without the consideration of multiple DG operations. Therefore, it is reasonable to guess that the voltage regulation performance might be worse in the multiple DG operation than the single DG one. To simulate the multiple DG operation, the real power of each DG changes from zero to 0.25MW. Also, the reactive powers of the DGs change based on the P-Q droops of buses 09 and 23, respectively. In the case of controlled simulation, the reactive powers are maintained at zero. As shown in Figs. 7 and 8, the increased voltages in the controlled simulation are resolved by the reactive power absorption based on the P-Q droop. As guessed, the voltage drops get serious by two DGs operation. This is because total reactive power absorption increases compared to the single DG operation. Therefore, it becomes more important to estimate the nonlinear P-Q droop curve in the case of multiple DGs operation.

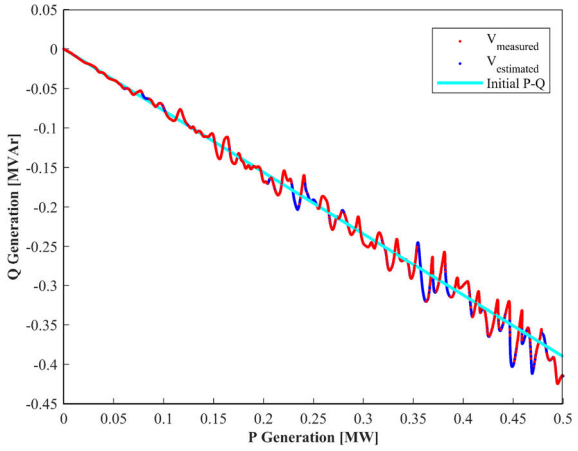

FIGURE 9. Real and reactive powers based on the initial P-Q curve (cyan), which are used for voltage measurement (red) and estimation (blue) in bus 23.

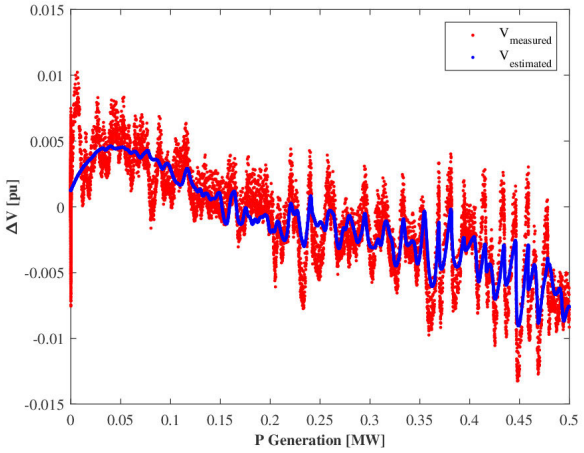

FIGURE 10. Measured voltage variations (red) and its estimation (blue) on bus 23.

VI. CASE STUDIES WITH NONLINEAR P-Q CURVE

A. SINGLE DG WITH NONLINEAR P-Q CURVE

To verify the performance of the proposed nonlinear P-Q curve estimation, a DG is connected to bus 23 in the power system of Fig. 2, representatively. The reactive power consumptions are controlled by adding small random noises to the initial P-Q ratio to minimize the unnecessary voltage variations while acquiring sufficient data for the estimation as shown in Fig. 9. Therefore, the amounts of the voltage variations (red in Fig. 10) do not exceed those in the case with zero reactive power (blue in Fig. 6) even if noises from other devices affected the voltage variations together. The y-axis of Fig. 10 shows the z-axis of Fig. 9 (i.e., direction from paper to reader). Those results are important for the DG operation in the practical power system. This is because the large changes of the reactive powers increase the voltage variations although they help to acquire good quality data.

The proposed estimation method successfully extracts the voltage variation caused by real and reactive powers of the

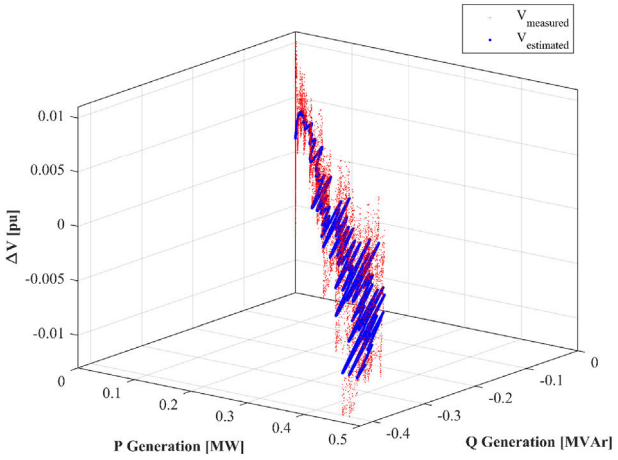

FIGURE 11. Measured (red) and estimated (blue) voltage variations according to real and reactive powers in bus 23.

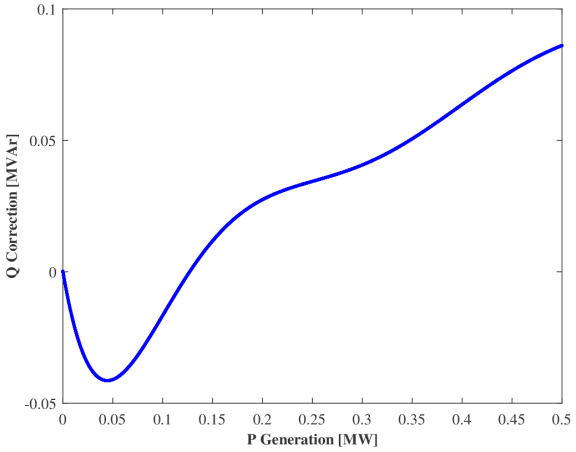

FIGURE 12. Reactive power correction concerning the initial P-Q droop by the nonlinear P-Q droop estimation in bus 23.

DG from that caused by other causes as shown in Fig. 10. The changes in the estimated ΔV are related to the reactive power changes as shown in Fig. 11. As the result of the estimation, the nonlinear P-Q curve is accurately acquired even if the samples are not acquired from wide operating range yet includes many voltage noises. The estimated voltage by the P-Q curve effectively rejects the voltage noises. It is shown in Fig. 12 that the reactive power correction curve concerning the initial P-Q droop in bus 23. Negative reactive power correction is required to be consumed when the real power injection is smaller than about 0.12MW. This is because the voltage increases when the initial P-Q curve is used (red in Fig. 6). By contrast, positive reactive power correction is required to be consumed when the real power injection is larger than about 0.12MW. This is because the voltage decreases when the initial P-Q curve is used (red in Fig. 6). The voltage variation is reduced by applying the modified nonlinear P-Q droop curve as the green line shown in Fig. 13. The blue line shows the worst voltage variation resulting from without Q control. The red line shows the modified

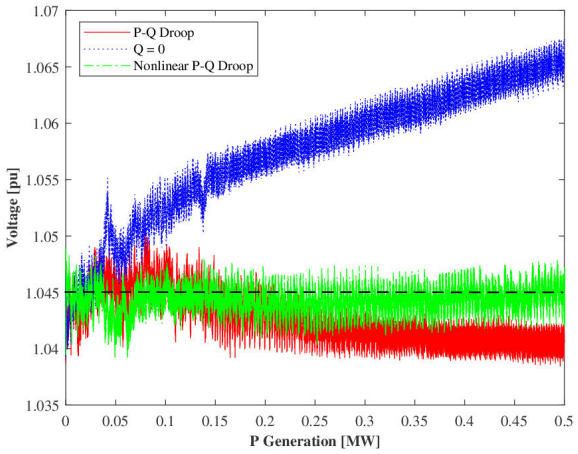

FIGURE 13. Reduction of voltage variation by nonlinear P-Q droop estimation in bus 23 (Dashed line means initial voltage with zero P and Q penetration).

voltage variation resulting from fixed P-Q droop control. The green line shows the best voltage profile resulting from the nonlinear P-Q droop control. Although the red line shows a similar performance to the green one, it has a positively bigger variation with at most 0.12MW of P and a negatively bigger variation with at least 0.12MW of P than the green one. This is thanks to the reactive power correction of Fig. 12 which composes the nonlinear P-Q droop control.

B. TWO DGs WITH NONLINEAR P-Q CURVE

To verify the performance of the proposed nonlinear P-Q curve estimation in the multiple DGs connected system, two DGs are connected to buses 9 and 23, respectively. In the same manner as the single DG-connected case, the reactive power consumptions are controlled by adding random changes to the initial P-Q ratios in buses 9 and 23, respectively. By contrast to the single DG-connected case, however, data for each DG should be acquired continuously during the system operation. This is because a DG cannot control the other DG's condition in a practical power system especially if the owner is different. The performance of the proposed method is representatively shown in Fig. 14. The red dots are measured data from bus 23. At first glance, it looks unclear what the measured data mean because many factors such as the multiple DGs and loads affect the voltage variations. Nevertheless, the proposed estimation method successfully extracts the meaningful relationship between voltage and powers as the blue dots. Those are the same at the DG on bus 9. As a result, it is mitigated the excessive voltage drops caused by two DGs operations with initial P-Q droop ratios (as shown in Figs. 15 and 16). The blue lines show the worst voltage variation resulting from without Q control. The red line shows the modified voltage variation resulting from fixed P-Q droop control. The green line shows the best voltage profile resulting from the nonlinear P-Q droop control.

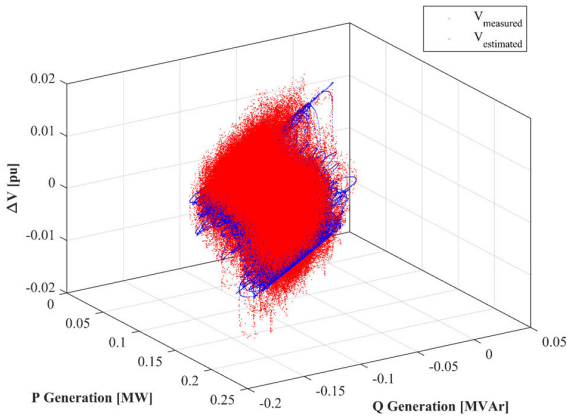

FIGURE 14. Measured (red) and estimated (blue) voltage variations according to real and reactive powers in bus 23 when two DGs are connected to buses 9 and 23, respectively.

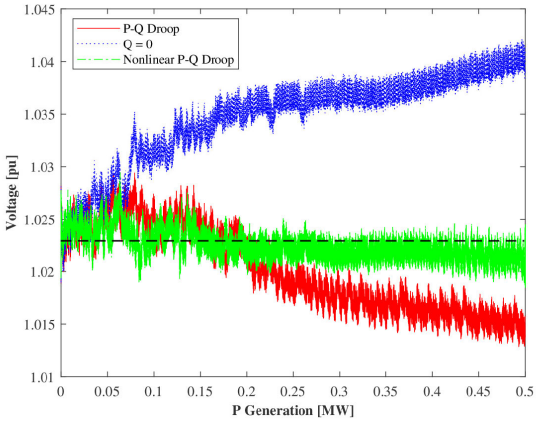

FIGURE 15. Reduction of voltage variation in bus 9 by nonlinear P-Q droop estimation based on data acquired during the power system operation (Dashed line means initial voltage with zero P and Q penetration).

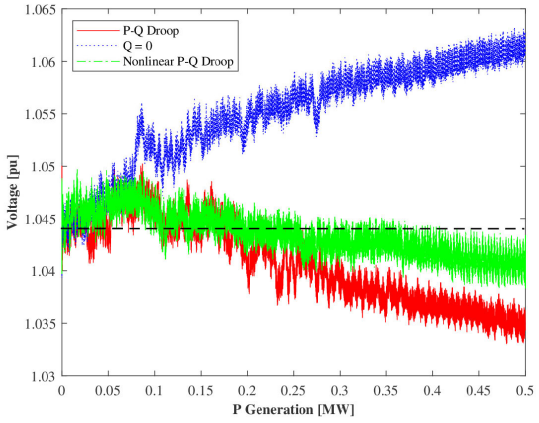

FIGURE 16. Reduction of voltage variation in bus 23 by nonlinear P-Q droop estimation based on data acquired during the power system operation (Dashed line means initial voltage with zero P and Q penetration).

C. ENTIRE BUS VOLTAGES

Although the main purpose of this paper is not to regulate the entire bus voltages but to mitigate the impact of real power penetration by optimally absorbing reactive power, it can also improve the entire bus voltage profile as an auxiliary effect as shown in Fig. 17. The maximum voltage maintains under 1.05pu so abiding by the grid code. In contrast, however, a few buses have voltages exceeding 1.05 pu when Q is zero as shown in Fig. 18.

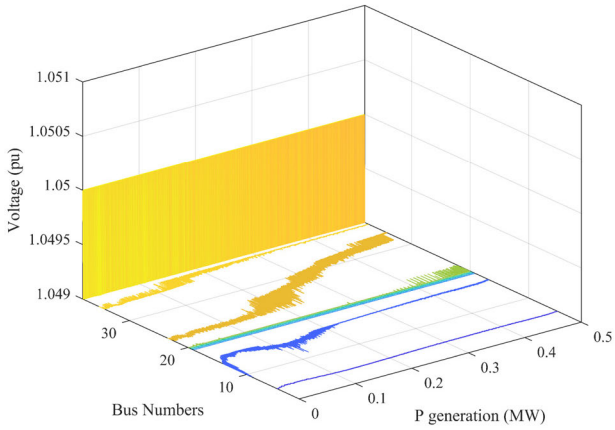

FIGURE 17. Sorted bus voltages in order of magnitude when proposed Q control is applied (The voltages above and below 1.049pu are shown in the 3D graph and the contour map, respectively).

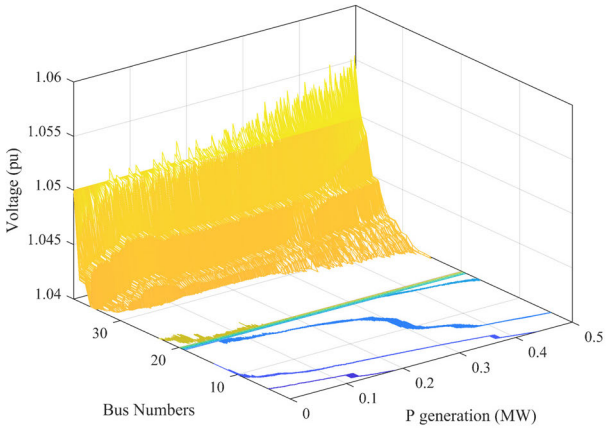

FIGURE 18. Sorted bus voltages in order of magnitude when Q of zero is applied (The voltages above and below 1.04pu are shown in the 3D graph and the contour map, respectively).

VII. CONCLUSION

This paper proposed the online nonlinear P-Q droop estimation of distributed generations based on the Kalman-filter algorithm to minimize the voltage variations that were caused by the real power penetrations of distributed generations (DGs). The P-Q droop is determined non-linearly based on the power system, not the individual device. Thus, this method is valid for any device that properly controls reactive power, regardless of type or sort.

To verify the performance of the proposed method, the estimated nonlinear P-Q droop curves were applied to the

TABLE 3. Island bus data in korea.

Bus No.	Bus Type	Voltage		Load		Generation	
		Mag. [pu]	Angle [rad]	P [MW]	Q [MVAR]	P [MW]	Q [MVAR]
1	S	1.050	0	0	0	0.576	0.057
2	PQ	1.042	-0.957	0	0	0.400	0.040
3	PQ	1.042	-0.968	0	0	0	0
4	PQ	1.036	-1.032	0	0	0	0
5	PQ	1.034	-1.049	0.093	0.009	0.050	0.005
6	PQ	1.034	-1.064	0	0	0	0
7	PQ	1.021	-1.166	0.022	0.002	0	0
8	PQ	1.021	-1.178	0.032	0.003	0	0
9	PQ	1.023	-1.358	0.038	0.004	0	0
10	PQ	0.986	-1.526	0	0	0	0
11	PQ	0.984	-1.536	0.010	0.001	0	0
12	PQ	0.982	-1.544	0.096	0.010	0	0
13	PQ	0.982	-1.540	0	0	0	0
14	PQ	0.982	-1.536	0.061	0.006	0	0
15	PQ	0.984	-1.525	0	0	0	0
16	PQ	0.999	-1.331	0.214	0.021	0.600	0.060
17	PQ	0.978	-1.578	0.323	0.032	0	0
18	PQ	1.042	-0.961	0	0	0	0
19	PQ	1.038	-1.003	0	0	0	0
20	PQ	1.038	-1.010	0.022	0.002	0	0
21	PQ	1.032	-1.087	0	0	0	0
22	PQ	1.030	-1.100	0.152	0.015	0.200	0.005
23	PQ	1.043	-1.262	0.029	0.003	0	0
24	PQ	1.009	-1.318	0.042	0	0	0
25	PQ	0.974	-1.669	0	0	0	0
26	PQ	0.972	-1.694	0.042	0.004	0	0
27	PQ	0.970	-1.721	0.160	0.016	0.050	0.005
28	PQ	0.970	-1.723	0	0	0	0
29	PQ	0.968	-1.743	0.084	0.008	0	0
30	PQ	0.970	-1.720	0.013	0.001	0	0
31	PQ	0.970	-1.718	0	0	0.050	0.005
32	PQ	0.968	-1.725	0	0	0	0
33	PQ	0.966	-1.746	0.029	0.003	0	0
34	PQ	1.034	-1.054	0.102	0.010	0	0
35	PQ	1.034	-1.046	0.069	0.007	0	0
36	PQ	1.032	-1.082	0	0	0	0
37	PQ	0.968	-1.724	0.144	0.014	0	0

DG models in the practical power system model and simulated by the electromagnetic transient program (EMTP). For the multiple DGs system application, the voltage and power data were acquired continuously during the DG operation and the nonlinear P-Q droop curves were estimated online. To minimize the voltage variation caused by reactive power manipulation for data acquisition, the initial P-Q droop curve was calculated based on the Jacobians in the steady state. Therefore, the proposed method could estimate the nonlinear P-Q droop curves successfully without excessive voltage variations during the data acquisition process. As a result, the voltage variation along with the real power penetration was remarkably reduced.

The proposed method makes the DG minimize its penetration impact by itself. The individual DG has a responsibility to its own impact, but not the other DG's. Therefore, it will contribute to minimizing the conflict caused between the independent power producers (IPPs). It means minimizing the IPPs' responsibility for market activity, yet also contributing to minimizing the system operators' burden.

It would be expected that the proposed online nonlinear P-Q droop estimation method is preferably utilized in power systems including renewable energy-based DGs, energy storage systems (ESSs), converter-based loads, etc.

APPENDIX

See Table 3.

REFERENCES

[1] V. M. Delmotte, P. Zhai, H. O. Pörtner, D. Roberts, J. Skea, P. R. Shukla, A. Pirani, W. M. Okia, C. Péan, R. Pidcock, S. Connors, J. B. R. Matthews, Y. Chen, X. Zhou, M. I. Gomis, E. Lonnoy, T. Maycock, M. Tignor, and T. Waterfield, *Special Report on Global Warming of 1.5 °C*, Oct. 2018.

[2] *Renewable Energy 3020*, Ministry Trade, Ind. Energy, Sejong, South Korea, Feb. 2017.

[3] S. C. Dhulipala, R. V. A. Monteiro, R. F. S. Teixeira, C. Ruben, A. Bretas, and G. C. Guimarães, "Distributed model-predictive control strategy for distribution network volt/VAR control: A smart-building-based approach," *IEEE Trans. Ind. Appl.*, vol. 55, no. 6, pp. 7041–7051, Nov. 2019.

[4] S. Sang, N. Gao, X. Cai, and R. Li, "A novel power-voltage control strategy for the grid-tied inverter to raise the rated power injection level in a weak grid," *IEEE J. Emerg. Sel. Topics Power Electron.*, vol. 6, no. 1, pp. 219–232, Mar. 2018.

[5] S. M. N. R. Abadi, A. Attarha, P. Scott, and S. Thiébaux, "Affinely adjustable robust volt/VAR control for distribution systems with high PV penetration," *IEEE Trans. Power Syst.*, vol. 36, no. 4, pp. 3238–3247, Jul. 2021.

[6] V. B. Pamshetti, S. Singh, and S. P. Singh, "Combined impact of network reconfiguration and volt-VAR control devices on energy savings in the presence of distributed generation," *IEEE Syst. J.*, vol. 14, no. 1, pp. 995–1006, Mar. 2020.

[7] A. Bidram, A. Davoudi, F. L. Lewis, and S. S. Ge, "Distributed adaptive voltage control of inverter-based microgrids," *IEEE Trans. Energy Convers.*, vol. 29, no. 4, pp. 862–872, Dec. 2014.

[8] G. Lou, W. Gu, Y. Xu, M. Cheng, and W. Liu, "Distributed MPC-based secondary voltage control scheme for autonomous droop-controlled microgrids," *IEEE Trans. Sustain. Energy*, vol. 8, no. 2, pp. 792–804, Apr. 2017.

[9] P. Jahangiri and D. C. Aliprantis, "Distributed volt/VAR control by PV inverters," *IEEE Trans. Power Syst.*, vol. 28, no. 3, pp. 3429–3439, Aug. 2013.

[10] E. Demirok, P. C. González, K. H. B. Frederiksen, D. Sera, P. Rodriguez, and R. Teodorescu, "Local reactive power control methods for overvoltage prevention of distributed solar inverters in low-voltage grids," *IEEE J. Photovolt.*, vol. 1, no. 2, pp. 174–182, Oct. 2011.

[11] Á. Molina-García, R. A. Mastromauro, T. García-Sánchez, S. Pugliese, M. Liserre, and S. Stasi, "Reactive power flow control for PV inverters voltage support in LV distribution networks," *IEEE Trans. Smart Grid*, vol. 8, no. 1, pp. 447–456, Jan. 2017.

[12] A. Safayet, P. Fajri, and I. Husain, "Reactive power management for overvoltage prevention at high PV penetration in a low-voltage distribution system," *IEEE Trans. Ind. Appl.*, vol. 53, no. 6, pp. 5786–5794, Nov. 2017.

[13] J. Hu, J. Zhu, D. G. Dorrell, and J. M. Guerrero, "Virtual flux droop method—A new control strategy of inverters in microgrids," *IEEE Trans. Power Electron.*, vol. 29, no. 9, pp. 4704–4711, Sep. 2014.

[14] W. Du, Q. Jiang, M. J. Erickson, and R. H. Lasseter, "Voltage-source control of PV inverter in a CERTS microgrid," *IEEE Trans. Power Del.*, vol. 29, no. 4, pp. 1726–1734, Aug. 2014.
[15] A. Singhal, V. Ajjarapu, J. Fuller, and J. Hansen, "Real-time local volt/VAR control under external disturbances with high PV penetration," *IEEE Trans. Smart Grid*, vol. 10, no. 4, pp. 3849–3859, Jul. 2019.
[16] D. Cao, J. Zhao, W. Hu, F. Ding, Q. Huang, and Z. Chen, "Attention enabled multi-agent DRL for decentralized volt-VAR control of active distribution system using PV inverters and SVCs," *IEEE Trans. Sustain. Energy*, vol. 12, no. 3, pp. 1582–1592, Jul. 2021.
[17] L. Wang, R. Yan, F. Bai, T. Saha, and K. Wang, "A distributed interphase coordination algorithm for voltage control with unbalanced PV integration in LV systems," *IEEE Trans. Sustain. Energy*, vol. 11, no. 4, pp. 2687–2697, Oct. 2020.
[18] Y. Hu, W. Liu, and W. Wang, "A two-layer volt-VAR control method in rural distribution networks considering utilization of photovoltaic power," *IEEE Access*, vol. 8, pp. 118417–118425, 2020.
[19] D. O. Amoateng, M. Al Hosani, M. S. Elmoursi, K. Turitsyn, and J. L. Kirtley, "Adaptive voltage and frequency control of islanded multi-microgrids," *IEEE Trans. Power Syst.*, vol. 33, no. 4, pp. 4454–4465, Jul. 2018.
[20] C. Zhang and Y. Xu, "Hierarchically-coordinated voltage/VAR control of distribution networks using PV inverters," *IEEE Trans. Smart Grid*, vol. 11, no. 4, pp. 2942–2953, Jul. 2020.
[21] S. Singh, V. B. Pamshetti, A. K. Thakur, and S. P. Singh, "Multi-stage multiobjective volt/VAR control for smart grid-enabled CVR with solar PV penetration," *IEEE Syst. J.*, vol. 15, no. 2, pp. 2767–2778, Jun. 2021.
[22] M. G. Kashani, M. Mobarrez, and S. Bhattacharya, "Smart inverter volt-watt control design in high PV-penetrated distribution systems," *IEEE Trans. Ind. Appl.*, vol. 55, no. 2, pp. 1147–1156, Mar. 2019.
[23] H. P. Corrêa, F. H. T. Vieira, and L. P. G. Negrete, "Double pilot node decentralized voltage control of PV generators via droop-type optimization-free reactive support," *IEEE Access*, vol. 10, pp. 109476–109487, 2022.
[24] D. Miller, G. Mirzaeva, C. D. Townsend, and G. C. Goodwin, "Decentralised droopless control of islanded radial AC microgrids without explicit communication," *IEEE Open J. Ind. Appl.*, vol. 3, pp. 104–113, 2022.
[25] H. Saadat, *Power System Analysis*. New York, NY, USA: McGraw-Hill, 2004, pp. 233–234.
[26] D. Choi, J.-W. Park, and S. H. Lee, "Virtual multi-slack droop control of stand-alone microgrid with high renewable penetration based on power sensitivity analysis," *IEEE Trans. Power Syst.*, vol. 33, no. 3, pp. 3408–3417, May 2018.
[27] J. Khodaparast, "A review of dynamic phasor estimation by non-linear Kalman filters," *IEEE Access*, vol. 10, pp. 11090–11109, 2022.
[28] Y. Bian, Z. Yang, X. Sun, and X. Wang, "Speed sensorless control of a bearingless induction motor based on modified robust Kalman filter," *J. Electr. Eng. Technol.*, vol. 18, Sep. 2023.
[29] H. Dong and Y. Wang, "Multi-vector robust model predictive current control for PMSM based on incremental model," *J. Electr. Eng. Technol.*, vol. 18, no. 5, pp. 3657–3669, Mar. 2023.
[30] S. H. Lee, "Non-linear P-Q droop curve estimation based on Kalman-filter algorithm to improve voltage stability," *Trans. Korean Inst. Electr. Eng.*, vol. 70, no. 3, pp. 439–446, Mar. 2021.

SOO HYOUNG LEE (Member, IEEE) received the B.S. and Ph.D. degrees in electrical engineering from the School of Electrical and Electronic Engineering, Yonsei University, Seoul, South Korea, in 2008 and 2012, respectively. From 2012 to 2014, he was a Postdoctoral Researcher with the School of ECE, Georgia Institute of Technology, Atlanta, GA, USA. From 2014 to 2018, he was a Senior Researcher with Korea Electrotechnology Research Institute, Uiwang, South Korea. From 2018 to August 2023, he was an Associate Professor with the Department of ECE, Mokpo National University, Mokpo, South Korea. Since September 2023, he has been an Associate Professor with the Division of Electrical, Electronic, and Control Engineering, Kongju National University, Cheonan-si, South Korea. His research interests include converter-based microgrids, optimal coordination of DGs, converter control for DGs, multilevel converters for low-voltage ac systems, and nonisolated dc–dc converters for high-voltage applications.

DONGHEE CHOI (Member, IEEE) received the B.S. and Ph.D. degrees in electrical engineering from the School of Electrical and Electronic Engineering, Yonsei University, Seoul, South Korea, in 2012 and 2017, respectively. From 2017 to 2018, he was a Postdoctoral Research Associate with the School of Electrical and Electronic Engineering, Yonsei University. He was one of few who had been selected for a Postdoctoral Training (Fostering Next-Generation Researcher Program, in 2017) with the National Research Foundation (NRF), South Korea. He was also a Manager with the Energy Storage System (ESS) Team, Smart Energy Unit, Future Convergence Business Office, Korea Telecom (KT), Seoul. He is currently an Assistant Professor of electrical and control engineering with the Division of Converged Electronic Engineering, Cheongju University, Cheongju-si, South Korea. His research interests include power system dynamics, power system stability, and operation and control and stand-alone microgrid operation.

SEUNG-MOOK BAEK (Member, IEEE) was born in Seoul, South Korea. He received the B.S., M.S., and Ph.D. degrees from the School of Electrical and Electronic Engineering, Yonsei University, Seoul, in 2006, 2007, and 2010, respectively. He was a Research Engineer with the KEPCO Research Institute, from 2009 to 2012. He is currently a Professor with the Division of Electrical, Electronic, and Control Engineering, Kongju National University, Cheonan, South Korea. His current research interests include power system dynamics, hybrid systems, optimization control algorithms, real-time simulation, flexible ac transmission system (FACTS) devices, renewable energy, and control of distributed generations.